AD-A071 162 ILLINOIS UNIV AT URBANA-CHAMPAIGN COORDINATED SCIENCE LAB F/G 9/3
A ROBUST CONTROL SYSTEM DESIGN.(U)
1979 J E ACKERMANN AFOSR-78-3633

UNCLASSIFIED AFOSR-TR-79-0743 NL

| OF |
AD
A071 162

END
DATE FILMED
8 -79
DDC

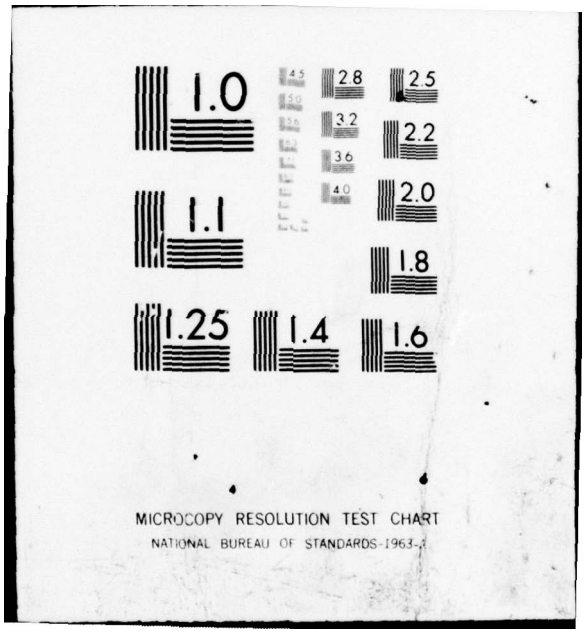
1.0
2.8
2.5
3.2
2.2
3.6
4.0
2.0
1.1
1.8
1.25
1.4
1.6
MICROCOPY RESOLUTION TEST CHART
NATIONAL BUREAU OF STANDARDS-1963-A

UNCLASSIFIED
SECURITY CLASSIFICATION OF THIS PAGE (When Data Entered)

AD A071162

DDC FILE COPY

REPORT DOCUMENTATION PAGE

READ INSTRUCTIONS BEFORE COMPLETING FORM

1. REPORT NUMBER: AFOSR-TR-79-0743	2. GOVT ACCESSION NO.
3. RECIPIENT'S CATALOG NUMBER	
4. TITLE (and Subtitle): A ROBUST CONTROL SYSTEM DESIGN	5. TYPE OF REPORT & PERIOD COVERED: Interim rept.
6. PERFORMING ORG. REPORT NUMBER	
7. AUTHOR(s): Juergen E. Ackermann	8. CONTRACT OR GRANT NUMBER(s): AFOSR-78-3633
9. PERFORMING ORGANIZATION NAME AND ADDRESS: University of Illinois, Coordinated Science Laboratory, Urbana, Illinois 61801	10. PROGRAM ELEMENT, PROJECT, TASK AREA & WORK UNIT NUMBERS: 61102F 2304/A1
11. CONTROLLING OFFICE NAME AND ADDRESS: Air Force Office of Scientific Research/NM, Bolling AFB, Washington, D.C. 20332	12. REPORT DATE: 1979
	13. NUMBER OF PAGES: 7
14. MONITORING AGENCY NAME & ADDRESS (if different from Controlling Office)	15. SECURITY CLASS. (of this report): UNCLASSIFIED
	15a. DECLASSIFICATION/DOWNGRADING SCHEDULE

16. DISTRIBUTION STATEMENT (of this Report)

Approved for public release; distribution unlimited.

17. DISTRIBUTION STATEMENT (of the abstract entered in Block 20, if different from Report)

DDC REPRINTED JUL 16 1979 RECEIVED C

18. SUPPLEMENTARY NOTES

19. KEY WORDS (Continue on reverse side if necessary and identify by block number)

097700

20. ABSTRACT (Continue on reverse side if necessary and identify by block number)

A representation of controllable linear systems is introduced, which permits assigning poles or characteristic parameters to a state feedback system by a matrix multiplication. This is used as a link between state space and classical parameter plane methods. The system representation maps a point in a $n^x p$ dimensional parameter space of characteristic parameters into the $n^x p$ dimemsional parameter space of state feedback gains, where p is the number of actuators. For p counts one the coordinates of the characteristic parameter space are the coefficients of the closed loop characteristic polynomial, for p greater than one —

(continued)

Unclassified

20. Abstract (continued)

they are coefficients in a characteristic polynomial matrix and its determinant is the characteristic polynomial. By this computationally simple mapping procedure it becomes feasible to map not only a fixed set of eigenvalues but also regions in the s or z plane, in which the eigenvalues shall be located. This relaxation of the dynamic specifications permits satisfying other typical design specifications like robustness with respect to sensor and actuator failures, large parameter variations, finite wordlength implementation, and actuator constraints. All tradeoffs between such requirements can be made in the feedback gain space. Three examples illustrate the variety of problems which can be tackled with this new tool.

word

12 JUNE 79

A ROBUST CONTROL SYSTEM DESIGN*

Juergen E. Ackermann
Coordinated Science Laboratory
University of Illinois, Urbana, Illinois 61801, USA

Abstract

A representation of controllable linear systems is introduced, which permits assigning poles or characteristic parameters to a state feedback system by a matrix multiplication. This is used as a link between state space and classical parameter plane methods. The system representation maps a point in a n×p dimensional parameter space $\mathcal{P}$ of characteristic parameters into the n×p dimensional parameter space $\mathcal{K}$ of state feedback gains, where p is the number of actuators. For p=1 the coordinates of the $\mathcal{P}$ space are the coefficients of the closed loop characteristic polynomial, for p > 1 they are coefficients in a characteristic polynomial matrix and its determinant is the characteristic polynomial. By this computationally simple mapping procedure it becomes feasible to map not only a fixed set of eigenvalues but also regions in the s or z plane, in which the eigenvalues shall be located. This relaxation of the dynamic specifications permits satisfying other typical design specifications like robustness with respect to sensor and actuator failures, large parameter variations, finite wordlength implementation, and actuator constraints. All tradeoffs between such requirements can be made in the $\mathcal{K}$ space. Three examples illustrate the variety of problems which can be tackled with this new tool.

1. INTRODUCTION

Control system specifications are usually not given in terms of a quadratic cost function or a set of eigenvalues. These are mainly used as free parameters in trial and error design procedures aimed at good tradeoffs between the dynamics of the system and other design aspects, for example actuator limitations and robustness with respect to sensor or actuator failures or other large parameter variations. Three questions in this context:

1. Quadruplex techniques (for example in aircraft control systems) are an expensive solution to the reliability problem. Is it not sufficient to guarantee that all unstable and insufficiently damped modes remain observable and controllable under all considered combinations of sensor and actuator failures?
2. Which system changes are so essential that they require adaptation of the control system by identification, failure detection etc.? Which range of such changes can be covered satisfactorily by fixed gain feedback or a few sets of gains and a simple switching criterion.
3. Is a given set of mixed specifications, e.g. on bandwidth and damping, actuator constraints, robustness requirements, etc., compatible within an assumed control system structure, or which of the specifications are conflicting, how far do we have to relax them?

This paper does not give a complete answer to these questions, however a method is proposed and some tools are provided to attack such questions under the following assumptions:

1. Only linear plants

$$\dot{\underline{x}} = \underline{A}\,\underline{x} + \underline{B}\,\underline{u} \qquad \underline{x} = [x_1 \ldots x_n]', \ \underline{u} = (u_1 \ldots u_p)' \quad (1)$$

or $\underline{x}(k+1) = \underline{A}\,\underline{x}(k) + \underline{B}\,\underline{u}(k)$ are considered. It is assumed that eq. (1) is written in "sensor coordinates," i.e. all measured variables are state variables x_i. Several pairs (A_1, B_1), (A_2, B_2), etc. may be given, e.g. for different operating points of an underlying nonlinear system. It is assumed that all pairs (A_i, B_i) are controllable and have the same controllability indices.

2. The price of an actuator is assumed to increase with

$$\bar{u}_i = \max|u_i(t)| \quad \text{and/or} \quad (2)$$

$$u_i' = \max|\dot{u}_i(t)| \quad (3)$$

where the worst initial state within given limitations is considered. $\bar{u}_i$ and/or u_i' should be kept "small."

3. A state feedback structure

$$\underline{u} = -\underline{K}'\underline{x} \quad (4)$$

is assumed. The details and examples are worked out for single input plants with

$$u = -\underline{k}'\underline{x} = -[k_1\ k_2\ \ldots\ k_n]\underline{x}. \quad (5)$$

For multi-input plants the basic result is stated in the Appendix. The n×p elements of $\underline{K}'$ are the free parameters of the proposed method. They are coordinates of a parameter space called "state feedback gain space" or "$\mathcal{K}$-space."

4. It is assumed that sensor and actuator failures occur in the form that the output of a failed element is not correlated to its input. Then the output is an external disturbance. Rejection of external disturbances is not considered in this paper. For the closed loop system

$$\dot{\underline{x}} = (\underline{A} - \underline{B}\,\underline{K}')\underline{x} \quad (6)$$

in sensor coordinates a failure of the ith sensor (actuator) is equivalent to a structural change by which the ith column (row) of $\underline{K}'$ becomes zero. Also in the case that a state variable is not measured, the corresponding column of $\underline{K}'$ is zero. It is part of the design to decide, which state variables are measured and for which of them redundancy must be provided for high system reliability. It is a goal to avoid failure detection and multiplexed components whenever possible.

5. It is assumed that the nominal dynamic behavior of the control system can be specified by a region in the eigenvalue plane - e.g. for a continuous time system in the s plane the region to the left of the boundary marked with σ=1 in Fig. 1 - where all eigenvalues must be located for the nominal structure and parameter values. For failure situations a relaxed "emergency specification," e.g. the boundary σ=0.5 or the

*This research was supported by the Deutsche Forschungs-und Versuchsanstalt für Luft-und Raumfahrt and by the U. S. Air Force under Grant AFOSR 78-3633.

Submitted through IEEE for the 1979 JACC

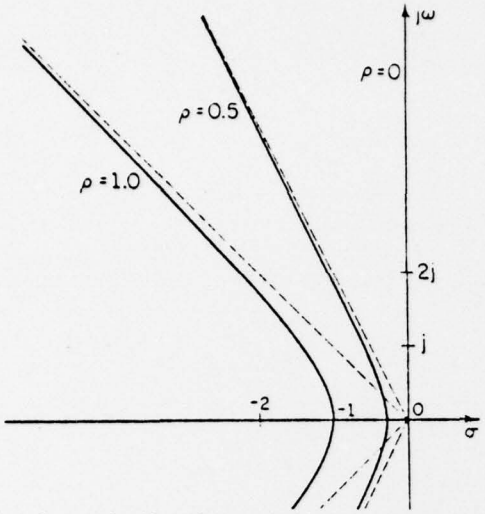

Fig. 1. A family of hyperbolic boundaries in s plane.

stability limit $\sigma=0$ in Fig. 1 may be given. A specification is robust under a failure if no eigenvalue crosses the corresponding boundary due to the failure.

The proposed method is: Design in $\mathcal{K}$-space. A region $\mathcal{K}_1$ in the $\mathcal{K}$-space is determined, such that all eigenvalues meet the specifications iff $\underline{k}' \in \mathcal{K}_1$. This may be the intersection of several such regions for different parameter values. Subsets of $\mathcal{K}_1$ with certain robustness properties can be found and tradeoffs with actuator constraints, bandwidth requirements, etc. can be made in the $\mathcal{K}$-space. The method also shows whether a solution exists under the given assumptions and if not, which alternatives exist for relaxation of specifications such that a solution will exist.

Parameter space methods have a long tradition, mainly in Russia and Yugoslavia. Siljak [1] gives a historical review of the work by Vishnegradsky, Neimark, Mitrovic, and others. Siljak generalized these parameter mapping methods significantly. A typical procedure for a continuous time system is to assume a controller structure with two free parameters α and β. Determine the closed-loop characteristic polynomial

$$P(s) = \sum_{i=0}^{n} p_i(\alpha,\beta)s^i = 0. \tag{7}$$

Substitute $s=\sigma+j\omega$ and separate eq. (7) into its real and imaginary parts: $Re(\sigma,\omega,\alpha,\beta)=0$, $Im(\sigma,\omega,\alpha,\beta)=0$. Assume these nonlinear equations have a solution

$$\alpha = \alpha(\sigma,\omega), \qquad \beta = \beta(\sigma,\omega). \tag{8}$$

Equation (8) allows to map σ,ω pairs on the boundary into the α-β-plane. The image boundaries divide the α-β-plane into regions characterized by the number of eigenvalues inside and outside the s-plane region.

In the present paper the control system structure is restricted to state feedback. This permits simplifying the determination of eq. (8) by pole placement methods. Consider for example a second order single-input system with $k_1=\alpha$, $k_2=\beta$ in eq. (5). In classical parameter plane methods $P(s) = \det(s\underline{I}-\underline{A}+\underline{b}\,\underline{k}') = p_0(\alpha,\beta)+p_1(\alpha,\beta)s+s^2=0$ is determined and with $s=\sigma+j\omega$ solved for α and β. In the method proposed in this paper the p_i are expressed in terms of σ and ω by

$$P(s) = (s-\sigma+j\omega)(s-\sigma-j\omega) = s^2-2\sigma s+\sigma^2+\omega^2$$
$$= p_0(\sigma,\omega)+p_1(\sigma)s+s^2 = 0. \tag{9}$$

Then by pole placement

$$k_1 = \alpha(p_0,p_1) = \alpha(\sigma,\omega)$$
$$k_2 = \beta(p_0,p_1) = \beta(\sigma,\omega). \tag{10}$$

Thus the mapping equation (8) is obtained in a different way. More generally for an nth order single input system in both approaches an n dimensional parameter space $\mathcal{P}$ with coordinates p_i is introduced as an intermediate step between the set of eigenvalues $\Lambda=\{\lambda_1 \dots \lambda_n\}$ and the $\mathcal{K}$-space. The relation between Λ and $\mathcal{K}$ can be expressed in both directions:

a) From $\mathcal{K}$ to $\mathcal{P}$ by the characteristic equation $P(\lambda)=\det(\lambda\underline{I}-\underline{A}+\underline{b}\underline{k}')$, from $\mathcal{P}$ to Λ by numerical factorization of $P(\lambda)$.
b) From Λ to $\mathcal{P}$ by multiplication of elementary factors $P(\lambda)=(\lambda-\lambda_1)(\lambda-\lambda_2)\dots(\lambda-\lambda_n)$, from $\mathcal{P}$ to $\mathcal{K}$ by pole placement.

In the next section pole placement is formulated in a form which makes direction b) far more attractive than direction a). In Section 3 the use of such boundaries for the design of robust control systems in $\mathcal{K}$-space is discussed. Section 4 shows the application to three examples.

2. BOUNDARY MAPPING

Pole-placement for single-input systems. The pole placement theorem is used in the form originally published in German in [2], available in English in [3]: Given an nth order monic polynomial $P(\lambda)$, an $n\times n$ matrix $\underline{A}$ and an $n\times 1$ vector $\underline{b}$ such that $\det \underline{R} \neq 0$, $\underline{R}=[\underline{b},\underline{A}\,\underline{b} \dots \underline{A}^{n-1}\underline{b}]$, the equation $P(\lambda) = \det(\lambda\underline{I}-\underline{A}+\underline{b}\,\underline{k}')$ has a unique solution and this solution is

$$\underline{k}' = \underline{e}'P(\underline{A}) \tag{11}$$

where $\underline{e}'$ is the last row of $\underline{R}^{-1}$.

With $P(\lambda) = (\lambda-\lambda_1)(\lambda-\lambda_2)\dots(\lambda-\lambda_n)$ (12)

$$= p_0+p_1\lambda+\dots+p_{n-1}\lambda^{n-1}+\lambda^n \tag{13}$$

eq. (11) may be written as

$$\underline{k}' = \underline{e}'(\underline{A}-\lambda_1\underline{I})(\underline{A}-\lambda_2\underline{I})\dots(\underline{A}-\lambda_n\underline{I}) \tag{14}$$
$$= \underline{e}'(p_0\underline{I}+p_1\underline{A}+\dots+p_{n-1}\underline{A}^{n-1}+\underline{A}^n). \tag{15}$$

For mapping from $\mathcal{P}$ space to $\mathcal{K}$ space it is more convenient to rewrite eq. (15) as

$$\underline{k}' = \underline{p}'\underline{E} \tag{16}$$
$$\underline{p}' = [p_0\ p_1 \dots p_{n-1}\ \ 1], \quad \underline{E} = \begin{bmatrix} \underline{e}' \\ \underline{e}'\underline{A} \\ \vdots \\ \underline{e}'\underline{A}^n \end{bmatrix}$$

$\underline{E}$ is an $(n+1)\times n$ matrix. If the inverse of eq. (16) is needed, it is convenient to express the last row of $\underline{E}$ by the Cayley-Hamilton theorem in terms of the previous rows. This however requires the evaluation of the characteristic polynomial $\det(\lambda\underline{I}-\underline{A}) = a_0+a_1\lambda+\dots+a_{n-1}\lambda^{n-1}+\lambda^n$. The invertible form of eq. (16) is

$$\underline{k}' = [p_0-a_0 \ \ p_1-a_1 \dots p_{n-1}-a_{n-1}]\underline{W}^{-1}, \quad \underline{W}^{-1} = \begin{bmatrix} \underline{e}' \\ \underline{e}'\underline{A} \\ \vdots \\ \underline{e}'\underline{A}^{n-1} \end{bmatrix} \tag{17}$$

The columns of $\underline{W}$ can be evaluated recursively by Leverrier's algorithm, which also gives the a_i [2].

The form (16) is most convenient for trial and error design procedures, graphical displays of cross-sections of the $\mathcal{K}$ space, etc. The plant description in the form of the matrix $\underline{E}$ is evaluated only once for a given pair $(\underline{A},\underline{b})$. The mapping of a trial design point in $\mathcal{K}$ space then requires n^2 multiplications and n^2 additions. This compares favorably with mapping a trial design point from the parameter space of quadratic criteria via the Riccati equation into $\mathcal{K}$ space. The generalization of eq. (16) to multiinput systems is given in the Appendix.

Sensitivities. The influence of a coefficient p_i of the characteristic polynomial on $\underline{k}'$, given the other p_j, follows from eq. (16) as

$$\frac{d\underline{k}'}{dp_i} = \underline{e}'\underline{A}^i. \tag{18}$$

The influence of an eigenvalue λ_i on $\underline{k}'$, given the other λ_j, follows from eq. (14) as

$$\frac{d\underline{k}'}{d\lambda_i} = -\underline{e}'(\underline{A}-\lambda_1\underline{I})\cdots(\underline{A}-\lambda_{i-1}\underline{I})(\underline{A}-\lambda_{i+1}\underline{I})\cdots(\underline{A}-\lambda_n\underline{I}) \tag{19}$$

For complex conjugate eigenvalues quadratic factors in $P(s)$ are more convenient. Let $P(\lambda) = (a+b\lambda+\lambda^2)Q(\lambda)$, then

$$\underline{k}' = \underline{e}'(a\underline{I}+b\underline{A}+\underline{A}^2)\cdot Q(\underline{A}) \tag{20}$$

$$\frac{d\underline{k}'}{da} = \underline{e}'Q(\underline{A}), \quad \frac{d\underline{k}'}{db} = \underline{e}'\underline{A}Q(\underline{A}). \tag{21}$$

Regions in λ plane. Boundaries, symmetric with respect to the real axis, in the λ plane will be specified, which describe the desired eigenvalue locations. Two cases will be discussed: A real root crossing a boundary or a complex conjugate pair crossing a boundary. The third possible case of roots leaving the region through infinity can be avoided by closing the contour by an arc of a circle with large radius. Typically the region is a connected set and the boundary has two intersections with the real axis. In this case there are two real root boundaries and one complex root boundary in $\mathcal{K}$ space. However other boundaries are possible, e.g. separate boundaries for slow and fast modes, etc. For each intersection of a boundary in the λ plane with the real axis at $\lambda=\sigma$, a real root boundary in $\mathcal{K}$ space is obtained from

$$P(\lambda) = (\lambda-\sigma)R(\lambda), \quad R(\lambda) = r_0+r_1\lambda+\cdots+r_{n-2}\lambda^{n-2}+\lambda^{n-1}. \tag{22}$$

By eqs. (16) and (22)

$$k_i = k_i(p_0\cdots p_{n-1}) = k_i(\sigma,r_0\cdots r_{n-2}) \quad i=1,2..n \tag{23}$$

where the k_i depend linearly on σ. Thus σ can be eliminated by one of the k_i's to give the linear boundary

$$k_j = k_j(k_i,r_0\cdots r_{n-1}) \quad j=1,2,\ldots,n, \quad j\neq i. \tag{24}$$

This is a straight line in the k_i-k_j plane. Another part of the boundary is obtained if a complex pair of eigenvalues crosses the boundary at $\lambda=\sigma+j\omega$. Then

$$P(\lambda) = (\lambda^2-2\sigma\lambda+\sigma^2+\omega^2)Q(\lambda)$$
$$Q(\lambda) = q_0+q_1\lambda+\cdots+q_{n-3}\lambda^{n-3}+\lambda^{n-2} \tag{25}$$

and the type of boundary in $\mathcal{K}$ space depends on the form of the boundary $\omega=\omega(\sigma)$ in the λ plane. For $\sigma=$ const., i.e. a parallel to the imaginary axis, the k_i are linear in ω^2. Thus for given q_i the image in the $\mathcal{K}$ space is a straight line.

Most commonly used boundaries are conic sections symmetric to the real axis, i.e.

$$\omega^2 = c_0+c_1\sigma+c_2\sigma^2. \tag{26}$$

Special cases are

$c_2<0$ ellipse, of particular interest are circles $c_2=-1$, e.g. constant natural frequency curves in s plane, stability limit and other boundaries in z plane.

$c_2=0$ parabola, or if also $c_1=0$, $c_0>0$ straight line parallel to the real axis.

$c_2>0$ hyperbola, in particular 2 straight lines for $\omega^2=c_2(\sigma-\sigma_0)^2$, $c_0>0$, e.g. constant damping lines in s-plane.

Figure 1 shows the family of hyperbolas

$$\omega^2 = -\rho^2+\sigma^2/\rho^2. \tag{27}$$

For $\rho\to 0$ this goes to the imaginary axis, for $\rho=1$ the asymptotes are the $1/\sqrt{2}$ damping lines. For a different scaling σ may be replaced by σ/d. Substituting eq. (26) into (25)

$$P(\lambda) = [\lambda^2-2\sigma\lambda+(1+c_2)\sigma^2+c_1\sigma+c_0]Q(\lambda). \tag{28}$$

This shows that the p_i and k_i depend linearly on σ for $c_2=-1$, i.e. for circular boundaries. Thus also in this case the boundaries in $\mathcal{K}$ space are straight lines if the eigenvalues in $Q(\lambda)$ are fixed and a complex pair of poles moves along the circle. For $c_2\neq -1$ the functions

$$p_i = p_i(\sigma,q_0\cdots q_{n-3}) \tag{29}$$

are quadratic in σ and by eq. (16) the same is true for

$$k_i = k_i(\sigma,q_0\cdots q_{n-3}). \tag{30}$$

One of these equations can be solved for $\sigma=\sigma(k_i)$, where only real roots $\sigma=\gamma\pm\delta$ are of interest. If only the left half λ plane branch of the conic section is needed, then $\sigma=\gamma-\delta$ is selected and substituted into the other k_i equations to give

$$k_j = k_j(k_i,q_0\cdots q_{n-3}), \quad i\neq j. \tag{31}$$

Note that this is not the curve in the k_i-k_j-cross-section of the $\mathcal{K}$ space, which would be obtained for $k_m=$const., $m\neq i,j$; eq. (31) gives the curve $k_j(k_i)$ for constant $q_0\ldots q_{n-3}$. For the numerical determination of boundaries in cross-sections of the $\mathcal{K}$ space the implicit form (30) is more useful. It gives σ-values as a parameter along the boundary. Constant damping spirals in the z plane are not conic sections. Usually they are supplemented by a condition $|z|<a$, $a<1$. The resulting regions can be reasonably well approximated by a family of nonintersecting circles

$$(v-v_0)^2+w^2 = r^2, \quad z = v+jw$$
$$v_0(v_0-1) = 0.99r(r-1), \quad v_0<0.5. \tag{32}$$

It is shown in Fig. 2. For $r=1$ it is the unit circle, with decreasing r the center v_0 of the circles moves to the right until it reaches 0.45 for $r=0.5$, it then goes back to zero, where $v_0=r=0$ is the deadbeat solution.

Regions in $\mathcal{K}$ space. Equations (22) and (25) show that the mapped boundaries in $\mathcal{K}$ space represent the conditions under which the number of eigenvalues inside and outside a λ-region can change. These $\mathcal{K}$-boundaries partition the $\mathcal{K}$ space into regions; each of them corresponds to a fixed number of eigenvalues inside the λ region, and it must be decided, for which $\mathcal{K}$ region all eigenvalues are inside the λ region. For closed contours in the λ-plane the $\mathcal{K}$ region is bounded, since by eq. (16) no k_i can go to infinity. If there are several bounded regions, a simple test is to check the eigenvalues for an arbitrary $\underline{k}'$ in the considered $\mathcal{K}$ region. An alternative are Siljak's "shading rules" for the boundaries [1].

Consider a second order system and a circular λ-region. Boundaries in the k_1-k_2-plane are three

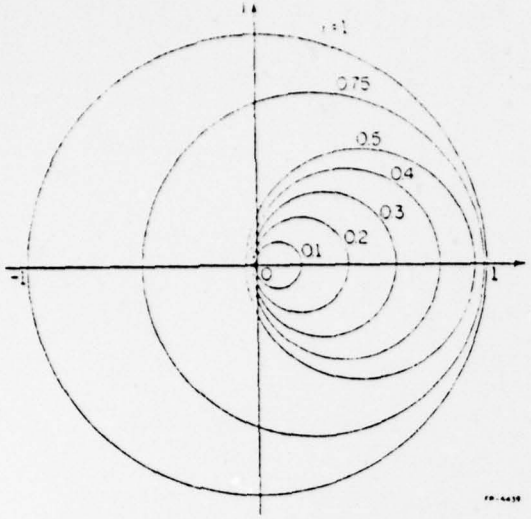

Fig. 2. A family of circular boundaries in z plane.

straight lines obtained for the two real root cases $\lambda=\tau_1$ and $\lambda=\tau_2$ and one complex root case. They partition the Ψ plane into seven regions with the properties: no pole outside the circle, one left, two left, one right, two right, one left and one right, complex outside. The only bounded region is the triangle, thus for k_1,k_2 in the triangle, λ_1 and λ_2 are inside the circle. At the vertices of the triangle both poles cross boundaries simultaneously. This is the case for 1) a double pole at τ_1, 2) a double pole at τ_2, and 3) one pole at τ_1 and one at τ_2. Thus the total mapping procedure consists of just three pole placements, i.e. twelve multiplications and twelve additions. This makes it easy to map the family of circles of Fig. 2. If the circle is deformed to a different closed contour with the same real axis intersections at τ_1 and τ_2, then the three vertices and two edges of the triangle remain unchanged, the third edge, i.e. the complex root boundary, is replaced by a curve. For a third order system and a circular λ-region the two real root boundaries are planes. The complex root boundary for a fixed real pole in a straight line. By moving the real pole the straight line moves and forms the third surface. The 4 vertices of the region are again obtained by pole placement of the four characteristic polynomials with zeros in the set $\{\tau_1,\tau_2\}$. For the corresponding region in Ψ space, Fam and Meditch [4] have shown that the convex hull of the region is the tetrahedron with the above mentioned vertices. By the linearity of the mapping equation $\underline{k}'=\underline{p}'\underline{E}$ this property does hold in the Ψ space also. Similarly for arbitrary n from [4] follows: The convex hull of the Ψ region, for which all eigenvalues are located inside a circle with center on the real axis and intersecting the real axis at τ_1,τ_2, is a polyhedron with n+1 vertices. They can be obtained by pole placement for the n+1 characteristic polynomials with zeros in the set $\{\tau_1,\tau_2\}$. The two real root hyperplanes are two of the surfaces of the polyhedron.

3. DESIGN IN Ψ SPACE

Robustness with respect to sensor failures. A specification is "F_i-robust" if it remains satisfied after a failure of sensor i, it is "F_{ij}-robust" if the same holds after failures of both sensors i and j. Fig. 3 shows an example of

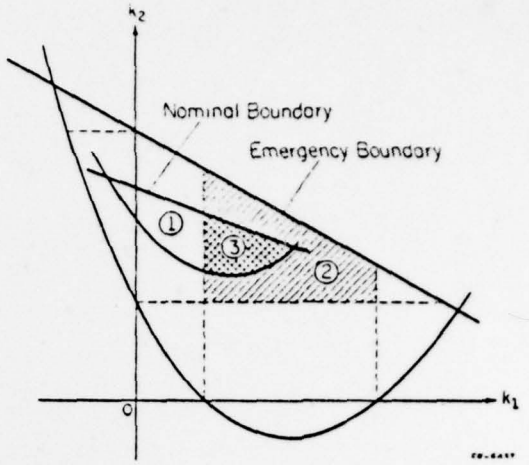

Fig. 3. Illustration of failure robustness and emergency boundaries.

boundaries in the k_1-k_2-subspace. It is assumed, that all other feedback gains are fixed. The projection of point 1 on the k_1 axis is outside the energency region, i.e. the emergency specification is not F_2-robust, it is however F_1 robust. Points 2 and 3 are F_1 and F_2 robust. No point is F_{12} robust since the origin $k_1=k_2=0$ lies outside the emergency region. Point 3 also meets the nominal specification and is a good candidate for a robust control system. Since the nominal boundary intersects the k_2 axis, an alternative to the robust solution 3 is to eliminate the x_1 sensor and to multiplex the x_2 sensor. This would maintain the nominal specifications under a failure ofone of the x_2 sensors. However it requires failure detection with at least three x_2 sensors and very likely is the more expensive solution.

Robustness with respect to actuator failures. Assume k_1 and k_2 in Fig. 3 are elements of different rows of the feedback matrix $\underline{K}'$ in eq. (A.8). Then the same arguments as above apply for the robustness of specifications with respect to actuator failures.

Robustness with respect to large parameter variations. Assume that for different operating conditions different pairs (A_1,B_1), (A_2,B_2) etc. are given. One boundary in the eigenvalue plane now maps into different boundaries in Ψ space, and it must be tested, whether there exists an intersection of the admissible regions. If it does not exist, then at least a gain scheduling system can be designed, in which each gain covers as many operating conditions as possible.

Robustness with respect to finite wordlength. The feedback control law may be implemented approximately in a short wordlength microprocessor as

$$\underline{u}+\Delta\underline{u}=(\underline{K}'+\Delta\underline{K}')(\underline{x}+\Delta\underline{x})\approx\underline{K}'\underline{x}+\Delta\underline{K}'\underline{x}+\underline{K}'\Delta\underline{x}. \qquad (33)$$

For small $\underline{x}$ the dominant term in $\Delta\underline{u}$ is $\underline{K}'\Delta\underline{x}$, i.e. the gains should be not too high. For large $\underline{x}$ the dominant term is $\Delta\underline{K}'\underline{x}$. The maximally $\Delta\underline{K}'$ robust solution is the center of the largest hypercube with edges parallel to the axes in the admissible Ψ-region. Fig. 4 illustrates $\Delta\underline{K}'$ robustness.

Actuator constraints. Constraints on $\bar{u}=\max|u(t)|$ and $\dot{u}=\max|\dot{u}(t)|$ can be treated in Ψ space. For the regulator problem

$$|u(t)|=|\underline{k}'\underline{x}(t)|\le\|\underline{k}\|\cdot\|\underline{x}(t)\| \qquad (34)$$

with equality for the worst case of $\underline{x}(t)$ (e.g., $\underline{x}=c\underline{k}$ for some $c\neq0$). Assuming that all state variables have been normalized to their maximum value,

the norm $\|\underline{k}\| = \sqrt{\underline{k}'\underline{k}}$ (35)

i.e., the distance from the origin in $\mathcal{K}$ space can be used as a measure for $\bar{u}=\max|u(t)|$. Similarly

$$|\dot{u}(t)| = |\underline{k}'\dot{\underline{x}}(t)| = |\underline{k}'(\underline{A}-\underline{b}\,\underline{k}')\underline{x}(t)|$$

and $|\underline{k}'(\underline{A}-\underline{b}\,\underline{k}')|$ can be used as a measure.

4. EXAMPLES

The following three examples of second, third, and fourth order show various typical design aspects and solutions in $\mathcal{K}$ space using the tools introduced in this paper. All calculations were done on a programmable pocket calculator.

Second order discrete system.

$$\underline{x}(k+1) = \underline{A}\,\underline{x}(k)+\underline{b}u(k), \quad \underline{A}=\begin{bmatrix}0 & -4\\ 1 & 4\end{bmatrix}, \quad \underline{b}=\begin{bmatrix}6/16\\ -5/16\end{bmatrix} \quad (36)$$

Find $u=-[k_1\ k_2]\underline{x}$ such that

i) stability is F_1-robust and, if possible, also F_2-robust,

ii) the system remains stable for $u=-[k_1\pm\Delta k, k_2\pm\Delta k]\underline{x}$ with the maximum Δk.

$$\underline{k}' = \underline{p}'\underline{E} = [p_o\ p_1\ 1]\begin{bmatrix}5 & 6\\ 6 & 4\\ 4 & -8\end{bmatrix} \quad (37)$$

The vertices of the stability triangle in the k_1-k_2-plane are determined by 3 pole placements

1. $P(z) = (z+1)^2 = z^2+2z+1$, $\quad \underline{k}' = [21 \quad 6]$
2. $P(z) = (z+1)(z-1) = z^2-1$, $\quad \underline{k}' = [-1 \quad -14]$ (38)
3. $P(z) = (z-1)^2 = z^2-2z+1$, $\quad \underline{k}' = [-3 \quad -10]$.

In Fig. 4 it is seen that the requirements for F_1 and F_2 robustness are not compatible, the F_1 robust region is chosen. ii) requires to place the largest square with sides parallel to the axes into the F_1 robust region. It has the center $\underline{k}'=[-0.454545 \quad -10.727272]$ and permits $\Delta k=1.454545$. This $\underline{k}'$ places the eigenvalues at $z_1=0.132$, $z_2=0.686$.

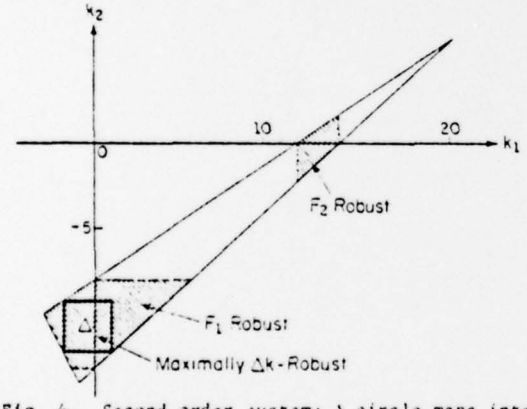

Fig. 4. Second order system: A circle maps into a triangle. Finite wordlength robustness.

DC servo motor. State variables in sensor coordinates are $\underline{x}=[\varphi\ \omega\ i]'$ with φ = shaft angle, ω = angular velocity, i = armature current, input: voltvoltage u. Assumptions: a) load torque $M_L = c\omega$, b) all state variables normalized to their maximal values, c) simple numerical values

$$\dot{\underline{x}} = \begin{bmatrix}0 & 1 & 0\\ 0 & -c & 1\\ 0 & -1 & -1\end{bmatrix}\underline{x} + \begin{bmatrix}0\\ 0\\ 1\end{bmatrix}u \qquad c>0 \quad (39)$$

d) state feedback $u = k_1(r-x_1)-k_2x_2-k_3x_3$, (40)

which gives a zero stationary error $\lim[r-x_1(t)]$ for a step reference input r, provided the system is stable. Find $\underline{k}'=[k_1\ k_2\ k_3]$ such that

i) stability is F_{23} robust for all loads c.

ii) For a load $c=2$ a complex pair of eigenvalues with damping $1/\sqrt{2}$ or more is required: Boundaries A and B in the s-plane of Fig. 5. This specification shall be F_2, F_3, and F_{23} robust.

iii) A tradeoff with the magnitude of $\bar{u}=\max|u|$ and the maximum bandwidth is to be made.

The observability analysis shows, that φ cannot be observed by ω or i, thus the φ sensor is essential, i.e. the reliability with respect to a failure of the φ sensor can be increased only by redundant φ sensors. The gain k_1 will be determined first. F_{23}-robustness of stability requires that $P(s) = s^3+(1+c)s^2+(1+c)s+k_1$, $c>0$, is Hurwitz, i.e. $0<k_1<(1+c)^2$. The worst case is $c\to 0$. For maximum bandwidth choose $k_1=1$.

$$\underline{k}' = \underline{p}'\underline{E} = [p_o\ p_1\ p_2\ 1]\begin{bmatrix}1 & 0 & 0\\ 0 & 1 & 0\\ 0 & -c & 1\\ 0 & -1+c^2 & -1-c\end{bmatrix} \quad (41)$$

i.e. $k_1=p_o=1$, $k_2=p_1-cp_2-1+c^2$, $k_3=p_2-1-c$. By eq. (25) $P(s)=(s^2-2\sigma s+\sigma^2+\omega^2)(q+s)=q(\sigma^2+\omega^2)+(\sigma^2+\omega^2-2\sigma q)s+(q-2\sigma)s^2+s^3$. $p_o=q(\sigma^2+\omega^2)=1$ guarantees $q>0$, i.e. the real eigenvalue is stable. For $c=2$ and boundary A, i.e. $\omega^2=\sigma^2$, $p_o=2q\sigma^2$, $p_1=2\sigma(\sigma-q)$, $p_2=q-2\sigma$ and by eq. (41) $k_1=2q\sigma^2=1$, $k_2=2\sigma(\sigma+2)-2q(1+\sigma)+3$, $k_3=q-2\sigma-3$. By $k_1=p_o=1$, $q=1/2\sigma^2$, the product of eigenvalues is fixed and $k_2=2\sigma(\sigma+2)-(1+\sigma)/\sigma^2+3$, $k_3=1/2\sigma^2-2\sigma-3$. This is curve A in Fig. 5. A Bode plot shows

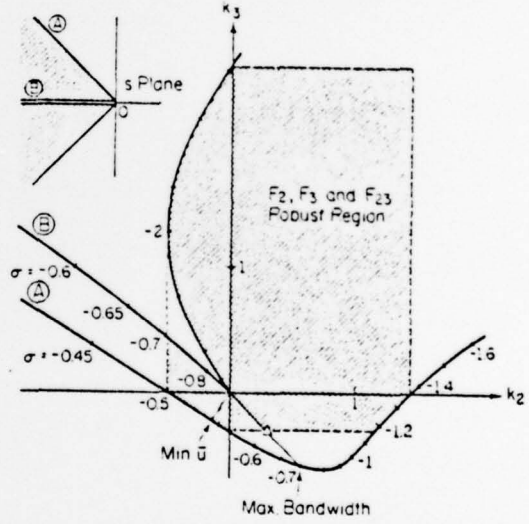

Fig. 5. Tradeoffs between tachometer (k_2) and amperemeters (k_3) feedback for a dc motor.

that the maximum bandwidth is obtained if real and complex poles have the same distance from the origin, i.e. $q=1$, $\sigma=-1/\sqrt{2}$, see Fig. 5. The minimum $\bar{u}$ is obtained at the point of curve A, which is closest to the origin.

For boundary B $P(s)=(s-\sigma)^2(s+q)=q\sigma^2+\sigma(\sigma-2q)s+(q-2\sigma)s^2+s^3$, and as before $k_2=\sigma(\sigma+4)-2(1+\sigma)/\sigma^2+3$, $k_3=1/\sigma^2-2\sigma-3$. Points in the shaded region satisfy specifications ii). The point of maximum bandwidth on the A curve is not in the robust region, therefore damping $>1/\sqrt{2}$ is necessary. If $q=1$ is kept constant and the complex poles move along the unit circle, then k moves along a straight line in the k_2-k_3-plane. Two points of this line are $k_2=k_3=0$ for a triple pole at $s=-1$ and the point $\sigma=-1/\sqrt{2}$ on curve A. Thus a good first choice would be the point $k_2=0.3$, $k_3=-0.3$ indicated by the triangle in Fig. 5.

Crane. Consider a crane with the physical parameters m_c=crab mass, m_L=load mass, ℓ=rope length. Its state variables are x_1=crab position, x_2=crab velocity, x_3=rope angle and x_4=rope angular velocity. For small rope angles the linearized state equations are

$$\dot{\underline{x}}=\begin{bmatrix}0 & 1 & 0 & 0\\ 0 & 0 & m_L g/m_c & 0\\ 0 & 0 & 0 & 1\\ 0 & 0 & -\omega^2 & 0\end{bmatrix}\underline{x}+\frac{1}{m_c}\begin{bmatrix}0\\ 1\\ 0\\ -1/\ell\end{bmatrix}u \qquad (42)$$

with $\omega^2=(m_c+m_L)g/m_c\ell$. Let $g=10 m/sec^2$ for operation on earth. Input u is the force accelerating the crab. Eigenvalues are $\{0,0,j\omega,-j\omega\}$. The observability analysis shows that x_1 is not observable by x_2, x_3 or x_4, thus the crab position sensor is essential. It was shown in [5] that x_2 must be measured or estimated, without x_2-feedback a stabilization is impossible.

Given: m_c=1000 kg, ℓ=10 m, maximum load 3000 kg, design a sampled-data controller

$$u(kT) = -\underline{k}'\underline{x}(kT) \qquad (43)$$

for the following specifications:

i) Consider a typical movement: Pick up a load at rest and drop it 10m away at rest again, i.e. initial state $\underline{x}=[10\ 0\ 0\ 0]'$, final state $\underline{x}=\underline{0}$. During this movement the required force should not exceed 5000 Newton.

ii) The amplitude of the load oscillation after 10 seconds should be small for two typical loads m_L of 3000 kg and 1000 kg.

iii) It is desirable to avoid the measurement of the rope angular velocity x_4.

The sampling interval T was selected such that in the worst case m_L=3000 kg the complex poles in z-plane lie on a 45° angle with respect to the positive real axis. This results in $T=\pi/8$.

The discretization and evaluation of the $\underline{E}$ matrix were done in center of mass coordinates, in which the system is block diagonalized. The result, transformed back to sensor coordinates $\underline{x}$, is then

$$\underline{E}=[\underline{E}_1 \quad a\underline{E}_1+\underline{E}_2] \qquad a=m_L\ell/(m_c+m_L) \qquad (44)$$

$$\underline{E}_1=\frac{(m_c+m_L)(2\sin\omega T-\sin 2\omega T)}{T^2\cdot(5\sin\omega T-4\sin 2\omega T+\sin 3\omega T)}\begin{bmatrix}1 & -3T/2\\ 1 & -T/2\\ 1 & T/2\\ 1 & 3T/2\\ 1 & 5T/2\end{bmatrix}$$

$$\underline{E}_2=\frac{-m_c\ell}{2\sin\omega T/2\,(5\sin\omega T-4\sin 2\omega T+\sin 3\omega T)}[\underline{v}_0\underline{v}_1\underline{v}_2\underline{v}_3\underline{v}_4]'$$

$$\underline{v}_i=\begin{bmatrix}\omega^2[\cos(i-1/2)\omega T-2\cos(i-3/2)\omega T+\cos(i-5/2)\omega T]\\ \omega[\sin(i-1/2)\omega T-2\sin(i-3/2)\omega T+\sin(i-5/2)\omega T]\end{bmatrix}$$

$i=0,1,2,3,4.$

Note that this form $\underline{E}=\underline{E}(m_L,m_c,\ell,T)$ could also be used to implement a gain scheduled control law $\underline{k}'=\underline{z}'\underline{E}=\underline{k}'(m_L,m_c,\ell,T)$, which keeps the eigenvalues constant.

In the first design step a first guess for $\underline{k}'$ is determined for m_L=3000kg only. First a partial pole placement is made by eq. (14), which gives a $1/\sqrt{2}$ damping to the pendulum motion without changing its natural frequency, i.e. a pole pair at $z_{1,2}=0.4876\pm j0.3026$. For the initial condition $\underline{x}(0)=[10\ 0\ 0\ 0]'$ the first control input is $u(0)=10\,k_1$, thus $k_1\leq 500$ (Newton/m) is necessary to meet specification i). For a fast response k_1=500 is chosen. After specifying two eigenvalues and one feedback gain there remains one free parameter, which is conveniently exhibited as a parameter on the root locus for the remaining two poles. Its complex part is a circle around z=1 with radius 0.1786, the intersection of this circle with the $1/\sqrt{2}$ damping spiral at $z_{3,4}=0.3657\pm j0.1177$ is chosen. This results in $\underline{k}'=[500\ \ 1927\ \ 7867\ \ -788]$.

The simulation shows that u(kT) does not exceed 5000 Newton. For the nominal load of 3000 kg the maximal amplitude after 10 seconds is 4.3% of the initial displacement. This first solution is however unsatisfactory for m_L=1000 kg, with a maximal amplitude of 12.3% after 10 seconds.

In the second design step primarily the solution for m_L=1000 kg must be speeded up. From the first solution only the values k_1=500 and k_2=1927 are kept and k_3 and k_4 are the free parameters of the second step. The four eigenvalues move with k_3 and k_4, they shall be kept however in the circle r=0.5 in Fig. 2. The circle maps into the 3000 kg boundary in the k_3-k_4 plane shown in Fig. 6.

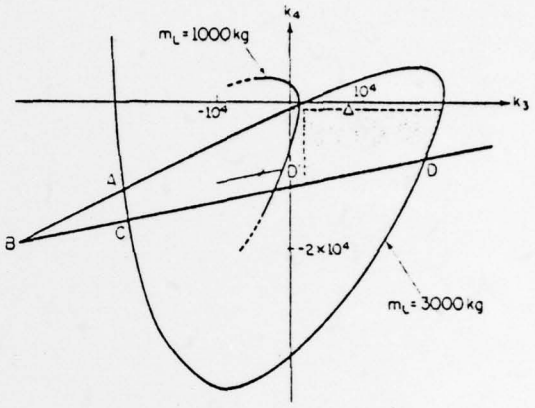

Fig. 6. A crane: Robustness with respect to large load variations.

At point A there are two different complex conjugate eigenvalue pairs crossing the circle simultaneously, such that the complex root boundary intersects itself. The right real boundary is outside the figure. At point B the complex and the left real root boundary for z_1=-0.05 meet, i.e. this k_3,k_4 pair generates a double pole at z=-0.05. In points C and D a complex pair and a real root at z=-0.05 cross the boundary simultaneously. The 1000 kg boundary has a similar shape, only its right part and the intersection D', corresponding to D, are shown. Thus the first design point indicated by the triangle must be moved to the left; let k_3=4000. Since k_4 is small anyway, k_4=0 is chosen in view of specification iii). Simulation shows that the maximum amplitudes after 10 seconds are 6.4% for 3000 kg and 3% for 1000 kg. The angle x_3 remains small, such that this assumption for the linearization of the plant equation is satisfied. If necessary a third design step could follow in which k_1=500 and k_4=0 are fixed and k_2 and k_3 are varied.

5. CONCLUSIONS

Classical parameter plane ideas have been combined with pole placement results to a design method in $\mathcal{Y}$ space. The crucial step is the introduction of a plant representation in the form of the matrix $\underline{E}$ in eqs. (16) and (A.5). The linear mapping from $\mathcal{P}$ space to $\mathcal{Y}$ space is performed by a multiplication with the matrix $\underline{E}$ and is thus reduced to a computationally very simple step. In $\mathcal{Y}$ space typical design aspects such as actuator limitations and robustness with respect to sensor and actuator failures, large parameter variations and short wordlength implementation have elementary geometric interpretations, and several questions of practical interest can be treated in a clear and simple way

as is illustrated by three examples.

The examples are restricted so far to tradeoffs in two free parameters at a time, where a graphical interpretation in cross-sections of the $\mathcal{Y}$ space is possible. This is already a practically applicable tool with apparent advantages over graphical one-parameter methods like root locus. For example in successively closing loops of a cascaded system it allows to make tradeoffs between two successive steps.

The concept of the method is however not limited in the number of parameters. Due to the computational simplicity of the mapping it seems feasible to develop computer-aided design methods with displays visualizing three-dimensional surfaces and regions by moving point of view or moving cross-section. If the computer has to make the tradeoffs in problems with many parameters, difficulties arise, if there does not exist a point in $\mathcal{Y}$ space satisfying all specifications. In this situation the concept of a moving boundary may be useful, which was used by Zakian and Al-Naib [6] in the numerical treatment of inequalities. In Figs. 1 and 2 this means that the parameter b or r is varied continuously until a solution is found.

6. REFERENCES

[1] Siljak, D. D., Nonlinear Systems, The Parameter Analysis and Design, J. Wiley, New York, 1969, Chapters 1 and 2.

[2] Ackermann, J., Abtastregelung (Sampled-data control), Springer, Berlin, 1972, pp. 310-312.

[3] Ackermann, J., "On the Synthesis of Linear Control Systems with Specified Characteristics," Automatica 13, pp. 89-94 (1977).

[4] Fam, A. T. and Meditch, J. S., "A Canonical Parameter Space for Linear Systems Design," IEEE Trans. AC-23, pp. 454-458 (1978).

[5] Ackermann, J., "Entwurf durch Polvorgabe," (Design by Pole Placement), Regelungstechnik 25, pp. 173-179 and 209-215 (1977).

[6] Zakian, V. and Al-Naib, U., "Design of Dynamical and Control Systems by the Method of Inequalities," IEE Proc. 120, pp. 1421-1427 (1973).

[7] Popov, V. M., "Invariant Description of Linear Time-Invariant Controllable Systems," SIAM J. Control 10, pp. 252-264 (1972).

APPENDIX

The generalization of eq. (16), $\underline{k}'=\underline{p}'\underline{E}$, to the multivariable case was published in [5] and is quoted here for easier reference:

Given a controllable pair $(\underline{A},\underline{B})$, let $\underline{B}=[\underline{b}_1 \dots \underline{b}_p]$ and

$$r_{ik}=\operatorname{rank}[\underline{B},\underline{A}\underline{B} \dots \underline{A}^{k-1}\underline{B},\underline{A}^{k}\underline{b}_1 \dots \underline{A}^{k}\underline{b}_i] \quad i=1,2\dots p$$
$$r_{ok}=r_{pk-1}. \tag{A.1}$$

A controllability index μ_i, i=1,2..p of the pair $(\underline{A},\underline{B})$ is the smallest integer k such that $r_{ik}=r_{i-1k}$. Then $\underline{A}^{\mu_i}\underline{b}_i$ is linearly dependent on the vectors left of it in the controllability matrix and can be expressed as

$$\underline{A}^{\mu_i}\underline{b}_i=-[\underline{B}\,\underline{A}\,\underline{B}\dots\underline{A}^{\mu_i-1}\underline{B}]\underline{z}_i=-[\underline{A}^{\mu_i}\underline{b}_1\dots\underline{A}^{\mu_i}\underline{b}_{i-1}]\underline{s}_i. \tag{A.2}$$

In order to make $\underline{s}_i=[s_{i1}\dots s_{ii-1}]'$ unique, let $s_{ij}=0$ if $\mu_j \le \mu_i$. Let

$$\underline{M}_{AB}=\begin{bmatrix} 1 & s_{21} & \cdots & s_{p1} \\ 0 & 1 & & \vdots \\ & & \ddots & s_{pp-1} \\ 0 & & 0 & 1 \end{bmatrix}. \tag{A.3}$$

Note that by Popov's theorem on feedback invariants [7], $\underline{M}_{AB}$ is invariant under a transformation $(\underline{A},\underline{B}) \to (\underline{T}(\underline{A}-\underline{B}\underline{K}')\underline{T}^{-1},\underline{T}\,\underline{B})$, $\det \underline{T}\neq 0$. Let

$$\underline{R}=[\underline{b}_1 \dots \underline{A}^{\mu_1-1}\underline{b}_1, \underline{b}_2 \dots \dots \underline{A}^{\mu_p-1}\underline{b}_p], \quad \underline{R}^{-1}=\begin{bmatrix}\underline{Q}_1 \\ \vdots \\ \underline{Q}_p\end{bmatrix} \tag{A.4}$$

and $\underline{e}_i'$ the last row of the $\mu_i \times n$ matrix $\underline{Q}_i$. Let

$$\underline{E}=\begin{bmatrix}\underline{E}_1 \\ \vdots \\ \underline{E}_p\end{bmatrix} \qquad \underline{E}_i=\begin{bmatrix}\underline{e}_i' \\ \underline{e}_i'\underline{A} \\ \vdots \\ \underline{e}_i'\underline{A}^{\mu_i-1}\end{bmatrix} \tag{A.5}$$

Introduce nxp characteristic parameters in a pxp matrix

$$\underline{P}'=\begin{bmatrix}\underline{p}_{11}' & \cdots & \underline{p}_{1p}' \\ \vdots & & \\ \underline{p}_{p1}' & \cdots & \underline{p}_{pp}'\end{bmatrix} \tag{A.6}$$

with $\underline{p}_{ii}'=[p_{ii0}\ p_{ii1} \cdots p_{ii\mu_i-1}\ \ 1]$

$\underline{p}_{ij}'=[p_{ij0}\ p_{ij1} \cdots p_{ij\mu_j-1}\ \ 0] \quad i\neq j$

$\underline{P}'$ generalizes $\underline{p}'$, the vector of coefficients of the characteristic polynomial, its coefficients p_{ijk} are the coordinates of an nxp dimensional parameter space $\mathcal{P}$. $\underline{P}'$ is related to the characteristic polynomial by

$$P(\lambda)=\det(\lambda\underline{I}-\underline{A}+\underline{B}\underline{K}')=\det[\underline{P}'\cdot\operatorname{diag}(\underline{\lambda}_i)],$$
$$\underline{\lambda}_i=[1 \ \lambda \dots \lambda^{\mu_i}]' \tag{A.7}$$

and to the state feedback matrix by

$$\underline{K}'=\underline{M}_{AB}\underline{P}'\underline{E}. \tag{A.8}$$

Thus the system representation $(\underline{E},\underline{M}_{AB})$ may be considered as a mapping between two nxp dimensional parameter spaces $\mathcal{P}$ and $\mathcal{K}$. Note that the n coefficients of any row of $\underline{P}'$ enter linearly into the determinant in eq. (A.7), thus they can be expressed by the coefficients of $P(\lambda)$ and by the remaining $n\times(p-1)$ characteristic parameters in $\underline{P}'$, which parameterize the remaining degrees of freedom after pole placement. If the coefficients of the first row of $\underline{P}'$ are eliminated in this way, eq. (A.8) results in n·p equations relating the feedback gains to the n(p-1) free parameters. Due to the structure of $\underline{M}_{AB}$, n(p-1) of these equations are linear, only the equations for the elements of the first row of K are nonlinear in the free parameters.

The free parameters can now be chosen according to additional requirements, e.g. minimizing the maximal feedback gain in view of actuator limitations or to make certain columns of $\underline{K}'$ equal to zero in order to save sensors.